Anomalous Segment Diffusion in Polydimethylsiloxane Melts

Stefan Pahl,† Gerald Fleischer,*,‡ Franz Fujara,† and Burkhard Geil†

Fachbereich Physik, Universität Dortmund, D-44221 Dortmund, Germany, and Fakultät für Physik und Geowissenschaften, Universität Leipzig, Linnéstrasse 5, D-04103 Leipzig, Germany

Received September 24, 1996; Revised Manuscript Received December 6, 1996[⊗]

ABSTRACT: Segmental diffusion in long-chain polymer melts has been measured by field-gradient NMR. An enlarged set of data and an improved data analysis leads to a modification of our previously published (*Macromolecules* **1994**, *27*, 4274) view. We now come to the following conclusions: In monodisperse polydimethylsiloxane (PDMS) melts, the self part of the intermediate scattering function stays almost Gaussian, that is $S(Q,t) \sim \exp[-Q^2D_{app}(t)t]$ for $t > 5 \times 10^{-3}$ s with an apparent self-diffusion coefficient whose time dependence is, within experimental accuracy, in accord with the reptation model. This is also the case for the molecular weight dependence of the long-time self-diffusion coefficient D_∞. However, the observed cross-over from anomalous to long time diffusion cannot be understood quantitatively within the strict reptation model.

1. Introduction

In the standard theory of polymer dynamics in the melt, the reptation theory, in the form of Doi and Edwards,[1] translational segmental dynamics is predicted to obey a power law dependence of the mean-square displacements $\langle r^2\rangle$ on the diffusion time t as $\langle r^2\rangle \sim t^\alpha$ with varying $\alpha(t)$ for increasing diffusion times. Following Doi−Edwards[1] one finds for increasing t: $\alpha = {}^1/_2$ (regime I), $\alpha = {}^1/_4$ (regime II), $\alpha = {}^1/_2$ (regime III), $\alpha = 1$ (regime IV). Other models and computer simulations[2−5] predict deviations from the above power law behavior.

Scattering experiments are a suitable tool for measuring the tagged segmental motion. In the case of the self part of the intermediate scattering function decaying like $S(Q,t) \sim \exp[-Q^2D_{app}(t)t]$ the measured self-diffusion coefficient $D_{app} = \langle r^2\rangle/(6t) \sim t^{\alpha-1}$ becomes t dependent itself thus containing the wanted information on $\alpha(t)$. The reptation model, however, does not precisely predict such a simple Gaussian behavior.[6] Measurements of $S(Q,t)$ may therefore not only serve to get $\alpha(t)$ but also to learn about the Q dependence of the dynamics.

Apart from incoherent quasielastic neutron scattering, which looks into the short time regimes I and II,[7] magnetic-field gradient NMR may be used as a suitable experimental tool to measure $S(Q,t)$ within the long time regimes III and IV.[8] A couple of NMR publications deal with this problem.[9−11] In our own work[12] preceding this study we demonstrated that the cross-over from long-range diffusion to anomalous diffusion for long-chain polymers like PDMS does indeed occur. But the time exponent $\alpha(t)$ observed for polybutadiene (PB) and polyisoprene (PI) deviated from $-{}^1/_2$ predicted by the Doi−Edwards theory.[1] It is the goal of the present work to present improved data and to analyze them more carefully by taking into account the "dipolar correlation effect" [13] which we did not consider before. The present procedure, which goes far beyond the previous one[12] as will be explained below, slightly modifies our conclusions on PDMS. Improved data on PB and PI will be presented in a forthcoming publication.

2. Theoretical Background

In this section we consider some aspects of the reptation model[1] in more detail. Fatkullin and Kimmich[6] have derived expressions for the spin−echo decay curves on the basis of the Doi−Edwards theory[1] in the different dynamic regimes II to IV for the motion of chain segments in entangled polymer melts. They considered the segmental displacements in the tube and the center-of-mass diffusion of the whole chain as uncorrelated and a temporally stable tube. In this work, we are concerned with the dynamic regimes III and IV. Therefore we use the expression derived in ref 6.

$$S(Q,t) = \exp\left(\frac{Q^4a^2\langle s^2(t)\rangle}{72}\right)\operatorname{erfc}\left(\frac{Q^2a\sqrt{\langle s^2(t)\rangle}}{6\sqrt{2}}\right)\exp(-Q^2D_\infty t) \quad (1)$$

with

$$\langle s^2(t)\rangle = \frac{6R_F{}^2}{a^2}\left(D_\infty t + \frac{a}{3}\sqrt{\frac{D_\infty t}{\pi}}\right) \quad (2)$$

Equation 2 holds in the time interval $T_R \ll t \ll T_d$, the regime III in the Doi−Edwards model. T_d is the tube disengagement time at which the cross-over to long-range diffusion of the center-of-mass of the chain takes place. T_R is the longest Rouse time of the chain[1] at which the cross-over from regime II to regime III occurs. $\langle s^2(t)\rangle$, the curvilinear mean square displacement of a segment along the tube, depends on three input parameters R_F, a, and D_∞. The parameter $R_F = \sqrt{N}b$ is the so-called Flory length, the end-to-end distance of the chain, and depends on the number of chain segments N and the segment length b. $a = \sqrt{N_e}b$ denotes the tube diameter with N_e being the number of segments between entanglements. D_∞ is the long-time self-diffusion coefficient of the center-of-mass motion of the chain. In the reptation model, D_∞ is proportional to M^{-2}. R_F and a can be obtained from independent experiments, values are known from literature. For times $t \gg T_d$ and for small Q values eq 1 reduces to

$$S(Q,t) = \exp(-Q^2D_\infty t) \quad (3)$$

The first two factors of eq 1 are nonexponential with

† Universität Dortmund.
‡ Universität Leipzig.
[⊗] Abstract published in *Advance ACS Abstracts,* January 15, 1997.

S0024-9297(96)01421-0 CCC: $14.00

respect to Q^2. However, their product shows only a weak nonexponentiality. In the experiments one has also to deal with the distribution of diffusivities in the sample due to the small polydispersity of the polymer. Therefore it is difficult to decide from the experiment whether an observed nonexponentiality of S vs Q^2 is to be attributed to a polydispersity of the sample or to the physical model outlined above.

The diffusivity can be determined experimentally from the initial slope of the curve log $S(Q,t)$ vs Q^2 which is equal to $D_{app}(t)t = \langle r^2(t)\rangle/6$, where $D_{app}(t)$ is a time-dependent apparent self-diffusion coefficient (see eq 11). On the other hand, one obtains from eqs 1 and 2

$$D_{app}(t) = D_\infty + \frac{\sqrt{2a^2\langle s^2(t)\rangle}}{6\sqrt{\pi}t}$$

$$= D_\infty + \frac{R_F}{\sqrt{3\pi}t}\sqrt{D_\infty t} + \frac{a}{3}\sqrt{\frac{D_\infty t}{\pi}} \qquad (4)$$

using $\mathrm{erfc}(x) \approx 1 - (2x/\sqrt{\pi})$ for small x.

We like to stress that the first two factors in eq 1 are derived for $t \ll T_d$ assuming the validity of the Doi–Edwards model with a temporally stable tube. Contour length fluctuations of the chain and finite lifetime effects of the tube have not been considered. The third factor $\exp(-Q^2D_\infty t)$ becomes 1 in this limit. As already stated above, this third factor dominates the decay of $S(Q,t)$ (eq 1) in the opposite limit $t \gg T_d$.

3. Experimental Method

The stimulated NMR echo S' [pulse sequence $(\pi/2)-\tau-(\pi/2)-t-(\pi/2)-\tau-$echo] in a strong static magnetic field gradient g is described in detail in refs 8 and 14 and the preceding publication.[12] Let us express the measured quantity S' here as follows:[13]

$$S'(g,\tau,t) \sim S_{diff}(g,\tau,t)\, S_1(t)\, S_2(\tau)\, S_{dip}(\tau,t) \qquad (5)$$

In this equation the following factors occur:

(a) The self correlation function of the (e.g.) protons

$$S_{diff}(g,\tau,t) = \langle \exp[-i\vec{Q}\vec{r}(0)] \exp[i\vec{Q}\vec{r}(t)]\rangle \qquad (6)$$

is the factor of interest, namely the incoherent part of the intermediate scattering function with a scattering vector $\vec{Q} = \gamma\cdot\vec{g}\cdot\tau$ (γ, gyromagnetic ratio; $\vec{g}$, magnetic field gradient vector; τ, evolution time = first pulse spacing).

(b) Spin–lattice relaxation

$$S_1(t) = \exp(-t/T_1) \quad \text{if exponential} \qquad (7)$$

(c) Spin–spin relaxation

$$S_2(\tau) = \exp(-2\tau/T_2) \quad \text{if exponential} \qquad (8)$$

(d) The dipolar correlation effect[13]

$$S_{dip}(\tau,t) \qquad (9)$$

which depends on τ and t but *not* on g. This effect stems from an incomplete averaging of dipolar couplings due to fast anisotropic local motions. It is particularly significant in entangled polymers and liquid crystals and leads to an echo damping due to slow segmental reorientations. In our present context we do not give explicit expressions for S_{dip}, which would need the specification of motional models and which are not necessary for our data evaluation.

In our prior publications we neglected the dipolar correlation effect. This is correct when local motions are isotropic over the relevant times t and the relevant length scale which is of order Q^{-1}. As has been pointed out by Kimmich[13] the dipolar correlation effect cannot be neglected in the case of entangled polymers where due to the local anisotropy of the segmental dynamics a residual dipolar coupling survives. Here we are only interested in the investigation of segmental displacements (diffusivities). We use the following procedure to get rid of the dipolar correlation contribution $S_{dip}(\tau,t)$ in our measurements and also of the relaxation terms $S_1(t)$ and $S_2(\tau)$.

In order to distinguish between $S_{diff}(g,\tau,t)$ and the other contributions we perform two experiments in different magnetic field gradients g_1 and g_2 but with identical times τ and t. Considering eq 5 we obtain

$$S(Q,t) = \frac{S'(g_1,\tau,t)}{S'(g_2,\tau,t)} = S_{diff}(g_{eff},\tau,t) \qquad (10)$$

The effective gradient is then given by $g_{eff} = \sqrt{g_1^2 - g_2^2}$ and $Q = g_{eff}\tau t$ if $S(Q,t) = \exp(-Q^2D_{app}t)$ is used (see eq 11 below). This Gaussian behavior is always observed within experimental accuracy. For $g_2 = 0$ we clearly get $g_{eff} = g_1$.

Our experiments have been performed in a specially designed gradient magnet[14] (Figure 1) at a proton Larmor frequency of $\omega_0/2\pi = 60$ MHz. By changing the height of the sample between two positions z_1 and z_2, where the resonance condition $\omega_0 = \gamma B_0$ is fulfilled, the two gradients of $g_1 = 185$ to 190 T/m and $g_2 = 25$ to 36 T/m (varying among different spectrometer settings) are attained. For checking the consistency, in some cases we have also performed experiments at 60 MHz in a homogeneous magnetic field ($g_2 = 0$ T/m).

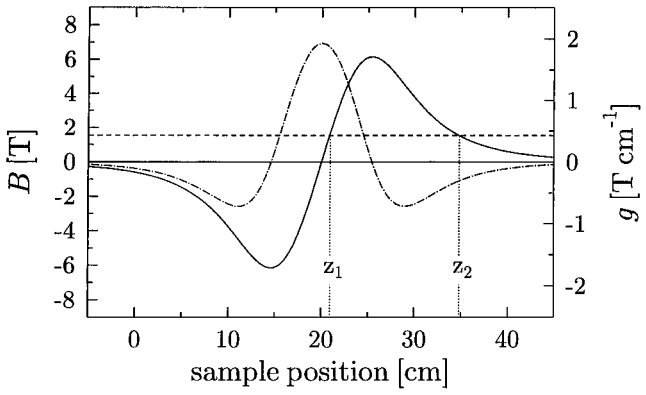

Figure 1. Magnetic field profile (—) and gradient (-•-) of the superconducting anti-Helmholtz type magnet. By choosing the appropriate sample position the wanted resonance field (- - -), corresponding to the spectrometer frequency of 60 MHz, is selected.

Table 1. Characteristic Sample Data

sample	M_w	M_D[c]	M_w/M_n	T (K)	R_F (nm)[d]	T_d (ms)[e]	D_∞ (10^{-14} m^2 s^{-1})[f]
1	118 000[a]	110 000	1.01	305	25	5	2.1
2	160 000[a]	149 000	1.03	305	29	14	1.0
3	344 000[a]	307 000	1.04	288	43	140	0.22
				305		114	0.27
				324		91	0.34
				345		79	0.39
4	716 000[b]	432 000	1.4	305	62	356	0.18

[a] Samples were purchased from Polymer Standards Service, Mainz, Germany. [b] Was made by the MPI für Polymerforschung, Mainz, Germany. [c] Diffusion average of molecular weights, see ref 16. [d] From $R_F^2 = 0.54 \times 10^{-20}\, M_w$ m^2;[18]. [e] $T_d = R_F^2/(6D_\infty)$. [f] As read from Figures 6 and 8.

4. Samples

Four high molecular weight polydimethylsiloxane (PDMS) samples with different molecular weights and different polydispersities are used in our study. Characteristic sample data are contained in Table 1. The

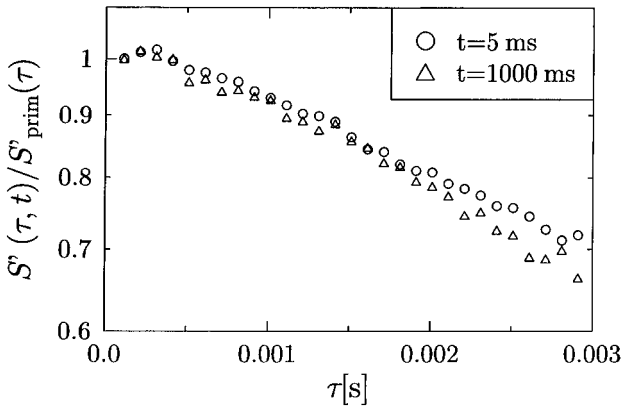

Figure 2. Stimulated echo divided by primary echo amplitude in sample 4 at two different diffusion times t in a homogenous magnetic field. As the division procedure cancels transverse relaxation effects, the decay of the curves indicates the presence of dipolar correlation effects. The temperature was $T = 305$ K.

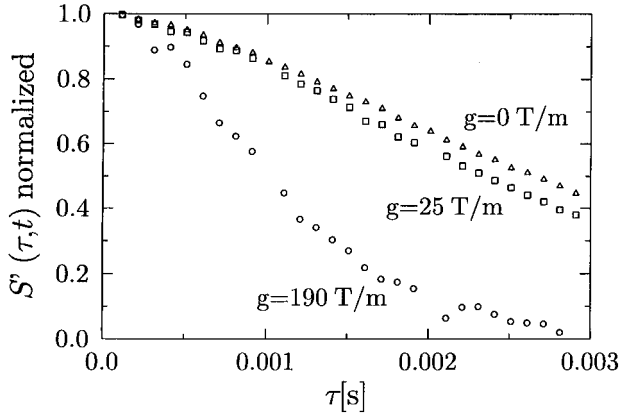

Figure 3. Stimulated echo decay in sample 3 for three different field gradients at $T = 305$ K and a diffusion time $t =$ 10 ms.

table also includes the temperature settings of the experimental runs described in this work.

5. Results and Discussion

5.1. Raw Data $S'(\tau,t)$. Figure 2 shows the measured ratio of the stimulated echo in zero gradient $S'(g = 0,\tau,t)[(\pi/2)-\tau-(\pi/2)-t-(\pi/2)-\tau-\text{echo}]$ and the primary zero gradient echo[13] $S'_{\text{prim}}(g=0,\tau)[(\pi/2)-\tau-(\pi/2)-\tau-\text{echo}]$ obtained in sample 4. The decay of this ratio is due to the dipolar correlation effect and will not be discussed further here. However, it is significant enough such that it must be taken into account for obtaining the correct diffusional contribution S_{diff}. Figure 3 presents the gradient dependence of typical stimulated echo decay curves also obtained in sample 3. Here we see that only the largest gradient leads to an appreciable extra decay, indicating the smallness of the diffusion coefficient. Again, the decay of the $g = 0$ curve (and mostly also of the 25−36 T/m curve) is mainly due to the dipolar correlation effect.

5.2. Normalized Data $S(\tau,t)$. As discussed above it is necessary to extract the diffusional part (eq 6) of the echo decay. Figure 4 shows echo decay curves $S(\tau,t)$ in sample 3 for two different diffusion times. The purpose of this plot is 3-fold: (1) It indicates the reduction of the statistical quality which stems from the normalization procedure (eq 10). (2) It clearly demonstrates that we deal with anomalous diffusion in the sense that the log S vs $\tau^2 t$ representation does not lead to a master

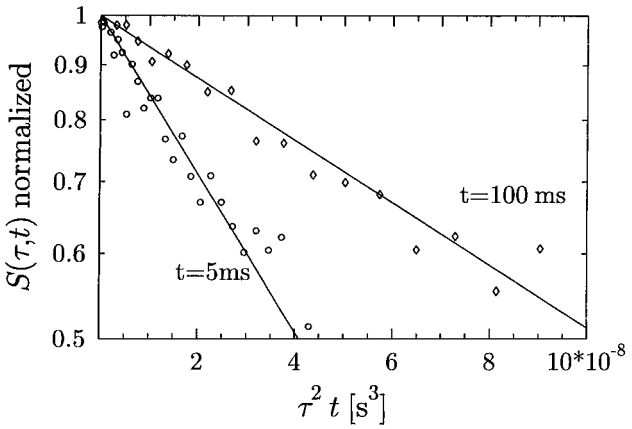

Figure 4. Semilogarithmic plot of the incoherent scattering function $S(Q,t)$ vs $\tau^2 t$ at two different diffusion times in sample 3. The temperature was $T = 305$ K. The fit curves indicate no significant deviations from a Gaussian behavior, eq 11.

curve which should be the case if the diffusion coefficient does not depend on the diffusion time t. Instead, for short diffusion times, the such-scaled curve decays faster than for long diffusion times. (3) From the semilogarithmic representation no clear deviation of the decay from Gaussian is seen within our statistical accuracy, i.e. $S(\tau,t) \sim \exp[-Q^2 D_{\text{app}} t]$ with $Q = \gamma g_{\text{eff}} \tau$ and a (time dependent) apparent self-diffusion coefficient D_{app}.

The latter point is of some importance since the reptation model does not necessarily lead to a Gaussian decay.[6,15] As already mentioned, the reptation motion as well as a distribution of chain lengths and therefore of diffusion coefficients lead to a nonexponentiality of $S(Q,t)$ vs Q^2. Even if the polydispersity of the sample is known, the distribution of the diffusion coefficients cannot be calculated since the relation between diffusion and molecular weight is not exactly known. The nonexponentiality of $S(Q,t)$ vs Q^2 stemming from the polydispersity is, however, expected to be small since our samples, with exception of sample 4, are rather monodisperse. Since no mathematical expression for the distribution of diffusion coefficients exists we rather pragmatically parametrized all measured PDMS decay curves by the Kohlrausch function $S(\tau,t) = \exp[-(\text{const}\ \tau^2)^{\beta}]$. In this way we obtained the stretching parameter β, the deviation from unity of which is a reasonable measure for the (non)exponentiality of $S(\tau,t)$ (Figure 5). It is seen from Figure 5 that three of the four PDMS samples are fitted with β values close to 1 such that a representation of the data by

$$S = S_0 \exp[-Q^2 D_{\text{app}}(t) t] \qquad (11)$$

is indeed reasonable. Only the sample 4 with its higher poldispersity leads to β values which more strongly deviate from unity.

5.3. Apparent Self-Diffusion Coefficient D_{app}. Figure 6 summarizes our results for $D_{\text{app}}(t)$ obtained from fits with eq 11 for all PDMS samples at one fixed temperature. The figure is instructive in several respects: Coming from long times, the data exhibit a cross-over from t-independent behavior to a time-dependent D_{app} (cross-over from regime IV to regime III). For the samples 2 and 3 the regime III is just reached. The $D_{\text{app}} \sim t^{-1/2}$ behavior in regime III is consistent with our data. Discrepancies, as stated in our previous publication[12] no longer seem to exist with this improved data treatment. However, the Rouse time

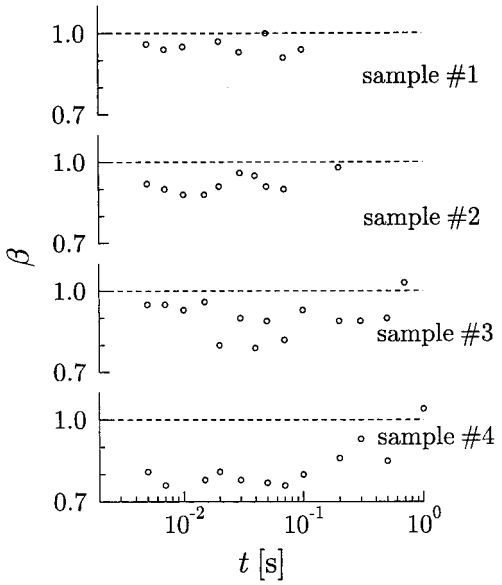

Figure 5. Stretching exponent β from Kohlrausch fits $S(\tau,t) \sim \exp[-(\text{const}\ \tau^2)^{\beta}]$ at $T = 305$ K.

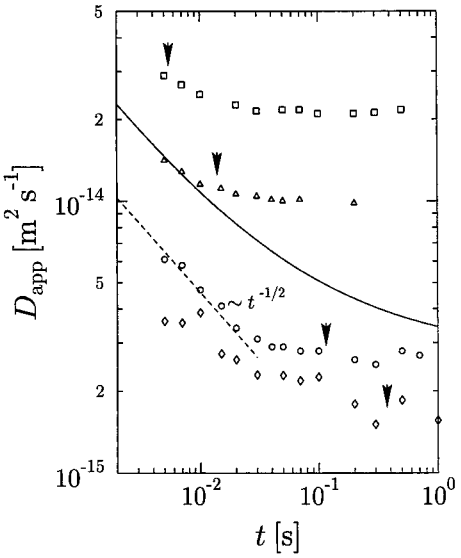

Figure 6. Time-dependent self-diffusion coefficients in PDMS with various molecular weights (□, sample 1 ($M_w = 118\,000$); △, sample 2 ($M_w = 160\,000$); ○, sample 3 ($M_w = 344\,000$); ◇, sample 4 ($M_w = 716\,000$)) at $T = 305$ K. The data were obtained by fits with eq 11. The dashed straight line indicates the reptation model prediction $D_{app} \sim t^{-1/2}$ in regime III. The full line is calculated with eq 4 for sample 3. The arrows indicate T_d (see Table 1).

T_R of sample 3 at which the cross-over to regime II occurs is $T_R = 4$ ms ($T_R = T_d M_e/M$ with $M_e = 12\,000$, the entanglement molecular weight). The time interval between T_R and T_d is not very large. In regime II, $D_{app} \sim t^{-0.75}$ is expected according to Doi−Edwards. Therefore, the (negative) time exponent of D_{app} should more or less smoothly increase between T_d and T_R. In the data of Fischer et al.[15] obtained with a polyethylene oxide sample of nominal molecular weight of 5×10^6 a slight decrease of the (negative) time exponent of D_{app} with decreasing diffusion time is evident, but the absolute value of D_{app} is by no means in accord with diffusion coefficients expected for this polymer.

5.4. Comparison with the Reptation Model. In this section we want to compare our findings with some of the predictions of the tube reptation model. The cross-over time T_d, from regime III to regime IV in the reptation model, should depend on M like $T_d \sim M^3$. Due to the broad cross-over and the limited experimental accuracy this relation cannot be checked. In Figure 6 the T_d values given in Table 1 are indicated by arrows. The long-time D_∞ scales like $D_\infty \sim M^{-2}$, where the "diffusion average" M_D (see Table 1) of the molecular weight should be used in the experimental verification if the diffusion coefficient is determined from the initial slope of ln $S(Q,t)$ vs Q^2.[16] We find a similar curve as reported in ref 17 for the same samples, but after correction for the different temperatures with an activation energy of 15 kJ/mol, our values of D_∞ are a factor of 0.6 below those of ref 17. This difference may be attributed to the calibration of the field gradient of one or both spectrometers.

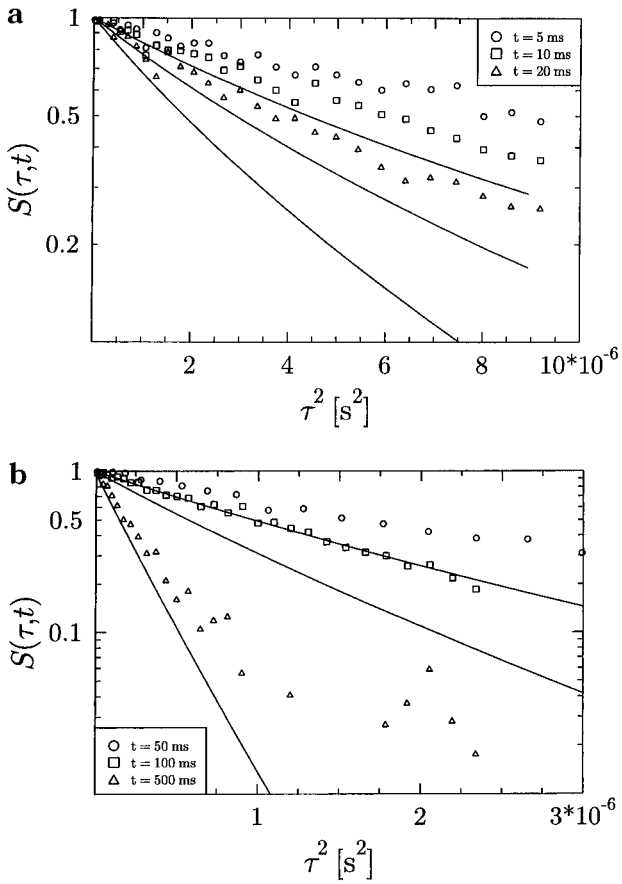

Figure 7. Normalized decay curves $S(\tau,t)$, sample 3, $T = 305$ K, and comparison with the reptation model (full curves), eqs 1 and 2, using the parameters $R_F = 43$ nm, $a = 6.5$ nm, and $D_\infty = 2.7 \times 10^{-15}$ m^2 s^{-1}; see Table 1 and text.

As discussed in section 5.2, it seems reasonable to analyze $S(Q,t)$ in terms of a Gaussian propagator (eq 11). Nevertheless, we now go a step further and test the validity of the Doi−Edwards model by comparing our experimental data with the curves obtained from eq 1. We make use of the fact that all of the three parameters are known, namely $R_F = 43$ nm (see Table 1), $a = 6.5$ nm,[7] and D_∞ from our own data (Figures 6 and 8, see also Table 1). Fixing these parameters and calculating eq 1, one immediately sees that the theoretical curves clearly do not fit the experimental $S(Q,t)$ anywhere (see Figures 7a,b, sample 3 at $T = 305$ K). In Figure 6, D_{app} calculated with eq 4 for sample 3 is shown. There is no accord with the experimental data. It is obvious that slight, physically permissible variations in none of the input parameters would improve the fits significantly. Hence, an overall consistency with

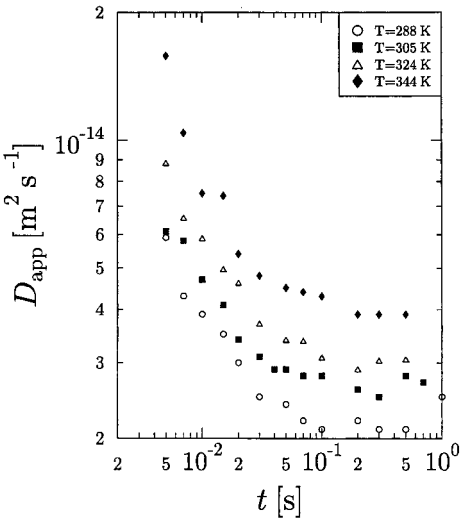

Figure 8. Time-dependent self-diffusion coefficients in sample 3 at various temperatures. The data were obtained by fits on eq 11.

the reptation model is missing in the time interval investigated by us.

5.5. Activation Energy. For sample 3 we have performed temperature-dependent measurements (Figure 8). Due to the broad cross-over exact values for T_d again cannot be derived, but the tendency for decreasing T_d with increasing temperature is obvious. For long times ($t > T_d$) we obtain an activation energy $E_A \approx 10$ kJ/mol. This is in contrast to a value obtained from viscosity measurements ($E_A = 15$ kJ/mol).[19] We note that the coupling model of Ngai et al. predicts a higher activation energy of shear viscosity in comparison with self-diffusion.[20] For times $t \ll T_d$, in regime III, the activation energy should be reduced by the factor of $^1/_2$ according to the Doi−Edwards theory (eq 5). This cannot be confirmed with our measurements. The calculated activation energy stays almost constant over the whole observed range. One should have in mind that we are still in the cross-over region from regime IV to III.

6. Conclusions

We have measured the self-diffusion of PDMS samples in the time regimes III and IV (after Doi−Edwards[1]) with field-gradient NMR. In the data evaluation the dipolar correlation effect[13] was properly taken into account. For the data evaluation the improved expressions from Fatkullin and Kimmich[6] derived on the basis of the Doi−Edwards theory[1] were used. In the regimes III and IV only the quantities R_F, a, and D_∞ enter into the formulae; therefore, no fit of the measured $S(Q,t)$ with the expressions of Fatkullin and Kimmich is necessary to compare the experimentally measured D_{app} with the theoretical expressions. R_F and a are known from separate experiments; D_∞ was measured in this work. The cross-over from the center-of-mass diffusion at long times to anomalous diffusion at shorter times was observed for all of our samples. Due to the experimental uncertainties of the scaling of T_d, the cross-over time between regime IV and III, with the molecular weight could not be checked. The time exponent of D_{app} in regime III was in accord with Doi−Edwards; however, more and precise experimental data are necessary to confirm this accordance safely. The most important result is that the experimentally determined dependence of D_{app} on the diffusion time t is quantitatively not in agreement with the assumption of a temporally stable tube in the Doi−Edwards theory. Coming from short times, the free diffusion of the center-of-mass of the chains is reached at considerably shorter times than T_d. Already at times much smaller than T_d the tube fluctuates. A curvilinear restricted diffusion of the segments along a temporally stable tube does not extend up to this time region. This fact may be important in connection with explaining the discrepancy between self-diffusion and viscosity data of polymer melts.[21]

Acknowledgment. Professor R. Kimmich kindly pointed out to us the crucial role of the dipolar correlation effect not only by his publications but also in several personal discussions. His help strongly triggered our present progress. F.F. also likes to thank Dr. E. Fischer for further clarifying discussions on this matter. G.F. thanks the Deutsche Forschungsgemeinschaft (SFB 294) for financial support.

References and Notes

(1) Doi, M., Edwards, S. F. *The Theory of Polymer Dynamics*; Clarendon Press: Oxford, U.K., 1986.
(2) Ngai, K. L., Rendell, R. W., Rajagopal A. K., Teitler S. *N.Y. Acad. Sci.* **1985**, *484*, 150.
(3) Schweizer, K. S. *J. Non-Cryst. Solids* **1991**, *643*, 191.
(4) Kremer, K.; Grest, G. S. *J. Chem. Phys.* **1990**, *92*, 5071.
(5) Herman, M. F. *Macromolecules* **1992**, *25*, 4925.
(6) Fatkullin, N.; Kimmich, R. *Phys. Rev. E* **1995**, *52*, 3273.
(7) Richter, D.; Ewen, B.; Farago, B.; Wagner, T. *Phys. Rev. Lett.* **1989**, *62*, 2140.
(8) Fleischer, G.; Fujara, F. NMR as a generalized scattering experiment. In *NMR-Basic Principles and Progress*; Kosfeld R., Blümich B., Eds.; Springer-Verlag: Berlin, 1994; Vol. 30, p 159.
(9) Callaghan, P. T.; Coy, A. *Phys. Rev. Lett.* **1992**, *68*, 3176.
(10) Fleischer, G.; Fujara, F. *Macromolecules* **1992**, *25*, 4210.
(11) Rommel, E.; Kimmich, R.; Spülbeck, M.; Fatkullin, N. *Prog. Colloid Polym. Sci.* **1993**, *93*, 155.
(12) Appel, M.; Fleischer, G.; Kärger, J.; Fujara, F.; Chang, I. *Macromolecules* **1994**, *27*, 4274.
(13) Kimmich, R.; Fischer, E.; Callaghan, P.; Fatkullin, N. *J. Magn. Res. A* **1995**, *117*, 53.
(14) Chang, I.; Fujara, F.; Geil, B.; Hinze, G.; Sillescu, H.; Tölle, A. *J. Non-Cryst. Sol.* **1994**, *172−174*, 674.
(15) Fischer, E.; Kimmich, R.; Fatkullin, N. *J. Chem. Phys.* **1996**, *104*, 22.
(16) Fleischer, G. *Macromol. Chem. Rapid Commun.* **1985**, *6*, 463.
(17) Appel, M.; Fleischer, G. *Macromolecules* **1993**, *26*, 5520.
(18) Berry, G. C.; Fox, T. G. *Adv. Polym. Sci.* **1968**, *5*, 261.
(19) Dodgson, K.; Bannister, D. J.; Semlyen, J. A. *Polymer* **1980**, *21*, 663.
(20) Mc Kenna, G. B.; Ngai, K. L.; Plazek, D. J. *Polymer* **1985**, *26*, 1651.
(21) Pearson, D. S.; Fetters, L. J.; Verstrate, G.; von Meerwall, E. D. *Macromolecules* **1994**, *27*, 711.

MA961421X